Forebody Vortex Management for Yaw Control at High Angles of Attack

Dhanvada M. Rao*
Vigyan Research Associates, Inc., Hampton, Virginia
Cary Moskovitz†
North Carolina State University, Raleigh, North Carolina
and
Daniel G. Murri‡
NASA Langley Research Center, Hampton, Virginia

The yaw control potential of deployable forebody strakes at angles of attack above the effectiveness range of conventional rudder has been investigated. The strakes are conformally stored in the forebody and, when deployed, force asymmetric vortex shedding from the forebody, thereby generating a controlled yawing moment. The concept was explored through low-speed wind-tunnel tests on a conical forebody in isolation as well as in generic fighter configurations. Force and moment measurements, supplemented with circumferential pressure and flow visualization surveys on an isolated forebody model, provided insights into the vortex mechanisms generated by forced asymmetrical separations and their yaw control potential at angles of attack up to 80.

Nomenclature

C_ℓ = rolling moment coefficient (body axis)
C_m = pitching moment coefficient
C_n = yawing moment coefficient (body axis)
C_p = pressure coefficient
α = angle of attack, deg
β = angle of sideslip, deg
δ_s = strake deflection angle, deg
ϕ = forebody circumferential angle from windward meridian, deg
ϕ_s = strake circumferential position, deg

Introduction

CONSIDERABLE interest currently exists in the development of aerodynamic techniques to enhance the controllability of next-generation combat aircraft, particularly in the context of poststall maneuverability requirements. A well-known control deficiency that limits the maneuverability of current fighters is the loss of rudder effectiveness due to submergence of the vertical tails into the low-energy wing wake at high angles of attack. Frequently, this phenomenon occurs concurrently with the deterioration of directional stability on highly swept configurations. Therefore, consideration must be given to evolving alternate aerodynamic means of providing yaw control, as well as stability augmentation systems that eliminate directional instability.

This paper addresses the possibility of manipulating the steady-state vortex system characteristic of slender forebodies at high angles of attack for the purpose of generating controlled side forces well forward of the aircraft center of gravity, thus providing an alternative source of yawing moment when the rudder becomes degraded. This approach is suggested by the considerable aerodynamic potential of naturally occurring vortex asymmetry on slender bodies at high angles of attack (e.g., Ref. 1); the technical challenge is to harness this potential through practical means and convert it into precisely controllable yaw power. One approach to implementing this concept was demonstrated in Ref. 2, by the use of jet blowing on a forebody shape characterized by a high fineness ratio and a horizontally elliptical cross section. These geometric features are known to promote strong vortex asymmetry effects[3] that favor the application of fluid amplification principles represented by jet blowing. On forebody shapes not naturally prone to pronounced vortex asymmetry, however, a different vortex manipulation approach is required to generate effective yaw control.

An alternative concept herein proposed is based upon forcibly creating an augmented asymmetric vortex system regardless of the forebody shape and modulating the asymmetry to generate the desired yaw control. This concept is realized by means of deployable forebody strakes, as shown in Fig. 1. Narrow, sharp-edged strakes have been employed in the past on forebodies and fuselage aft ends to improve the high-angle-of-attack handling and spin characteristics by fixing separation and controlling the vortex shedding. The strakes in the present concept are pivoted along their length and deployed at command from their conformally stored position on the forebody. The sharp edge of the deployed strake not only forces crossflow separation at a desired circumferential location, but also amplifies the shed vorticity in comparison with the basic forebody characteristics. The vortex strength and its position relative to the forebody may be regulated within limits by varying the strake deflection angle. Two alternative modes of strake deployment are indicated in Fig. 1. *Asymmetric* deployment (i.e., one strake deployed at a time) will force a strong asymmetric vortex and thus generate a side force, controllable via strake deflection. *Simultaneous* deployment (i.e., both strakes deployed) will establish a symmetrical pair of augmented vortices, from which a controlled side force is generated via antisymmetric (or differential) strake deflection.

The circumferential location ϕ_s of the forebody strakes would seem to be an important variable governing the side-force development over a broad angle-of-attack range. Furthermore, the side-force modulation capability through the variation of the strake deflection angle δ_s is of interest from the viewpoint of control precision. The relative merits of the

Received Oct. 22, 1986; revision received Nov. 26, 1986.

*Vice President. Associate Fellow AIAA.
†Graduate Student. Student Member AIAA.
‡Aerospace Technologist. Member AIAA.

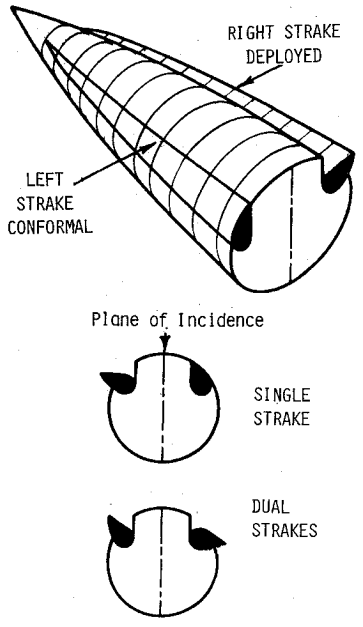

Fig. 1 Deployable forebody strake concept.

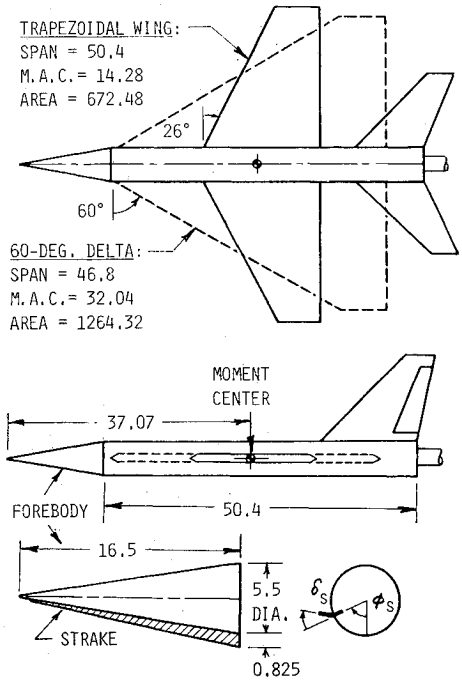

Fig. 2 Wind-tunnel model of generic fighter configurations (dimensions in inches).

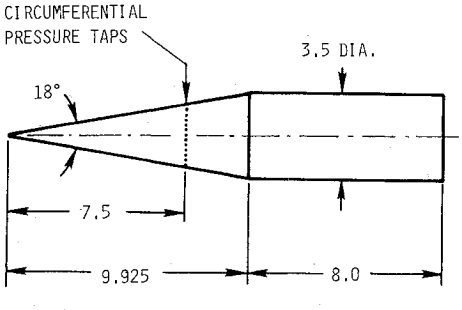

Fig. 3 Isolated forebody model for flow visualization and pressure surveys (dimensions in inches).

two aforementioned deployment options, viz., single or dual strakes, also need assessment. The foregoing parameters were initially addressed in an exploratory investigation of the deployable strake concept, using a cone-cylinder forebody for simplicity. The initial force and moment results have been reported in Ref. 4; this paper presents subsequently obtained results that emphasize the forebody flowfield aspects.

The low Reynolds number of the present study is to be noted. The crossflow separation and vortex characteristics of smooth and rounded slender bodies are known to be highly Reynolds number dependent[1]; however, highly three-dimensional, swept edge separations leading to spiral vortex sheets (viz., as with strakes) are generally regarded to be relatively less sensitive. In the case of asymmetric strake deployment, when free separation still occurs on one side of the forebody, Reynolds number effects must be anticipated. While the present results are believed to provide a valid assessment of the basic concept, they must of course ultimately be evaluated with respect to scale effects.

Experimental Details

The geometry and principal dimensions of the wind-tunnel model employed in this investigation are shown in Fig. 2. The generic fighter configurations were tested on a six-component strain gage balance in the NASA Langley 12-ft Low Speed Tunnel using standard instrumentation and data acquisition techniques. Two alternate flat-plate wing planforms, viz., a trapezoidal and a 60 deg delta, were tested on a common fuselage; the former configuration included the full empennage as shown, whereas the latter had only the vertical tail/rudder. The 9 deg semiangle conical forebody had longitudinal surface slots to hold sheet-metal strakes at selected ϕ_s positions. A set of strakes bent to different positive and negative δ_s angles was provided.

The isolated forebody pressure model (Fig. 3) was tested in the North Carolina State University (NC59) subsonic tunnel at a 50 deg angle of attack. In addition to pressure measurements with single and dual strakes in various ϕ_s and δ_s arrangements, this model also was used for crossflow visualizations. Noteworthy features of the present visualization technique are the use of a considerably thick (1 in.) light sheet for cross-plane illumination and helium bubbles rather than smoke for flow seeding. The camera was aligned to the model axis and long-exposure photographs taken showing bubble streaks traversing the cross plane and the steady-state vortex cores appearing as concentrated circular arcs. This somewhat unusual but straightforward adaption of a standard visualization technique greatly aided the understanding of the flow mechanisms underlying the present study.

The test Reynolds numbers in the various phases of this study, based on fuselage diameter, were as follows: NASA balance tests, 190,000; NCSU forebody pressures, 109,000; and NCSU flow visualization, 41,000.

Flowfield Characteristics

Some insight into the forced asymmetrical vortex characteristics due to forebody strakes can be gained through the coordinated flow visualization and circumferential pressure surveys obtained at a fixed angle of attack of 50 deg, selected results of which will be discussed here. For reference, the "basic" forebody (i.e., no strakes) data are presented in Fig. 4, which shows the vortex asymmetry expected when the angle of attack greatly exceeds the cone semiangles.

A comparison of single-strake deployment at $\phi_s = 60$ and 90 deg positions is presented in Fig. 5. These two strake positions generate fundamentally different types of asymmetry, as is evident in the corresponding circumferental pressure distributions. With $\phi_s = 60$ deg, the forced vortex produces a higher suction level on the strake side than that on the opposite (smooth) side of the forebody, which will produce a negative side force. Just the opposite is the case at $\phi_s = 90$ deg, i.e., a

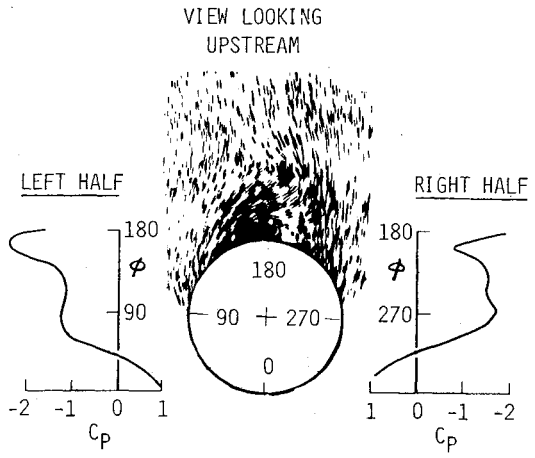

Fig. 4 Flow visualization and pressure distribution on basic forebody (strake off) at $\alpha = 50$ deg.

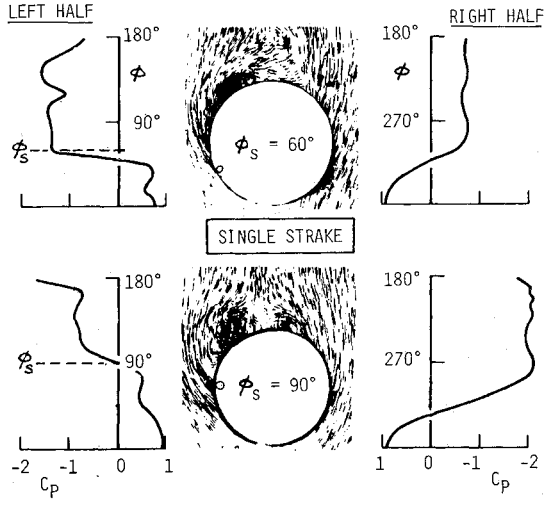

Fig. 5 Flow visualization and pressure distribution with single strake at $\phi_s = 60$ and 90 deg.

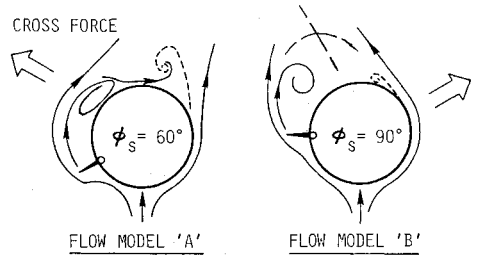

Fig. 6 Suggested crossflow models generating opposite side-forces with $\phi_s = 60$ and 90 deg.

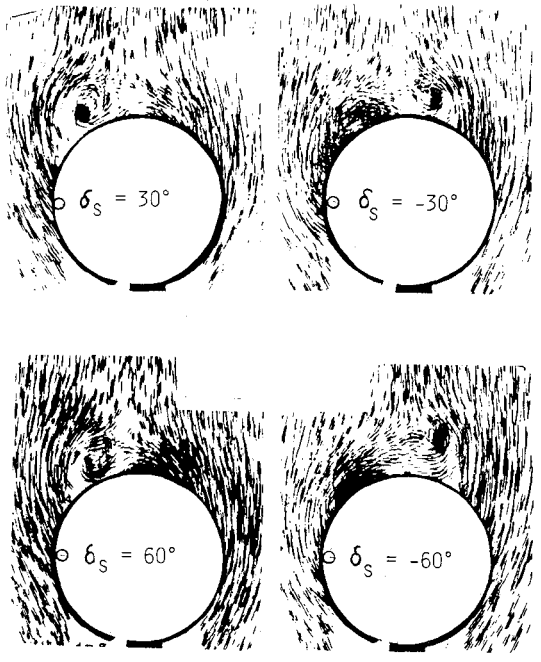

Fig. 7 Flow visualization with single strake at $\phi_s = 90$ deg, showing effect of strake deflection.

higher level of suction occurs on the smooth side, which will result in a positive side force.

The contrasting behavior with respect to strake position shown previously can be explained in terms of the interpreted vortex flow characteristics for the two cases as sketched in Fig. 6. At $\phi_s = 60$ deg, the strake vortex occurs close to the forebody and is followed by flow reattachement near the lee meridian. A significant portion of the left half of the forebody is covered by a shallow separation bubble, which may be considered to present a moving boundary in the direction of external crossflow. The result would be a clockwise circulation that tilts the cross-force vector to the left, thus generating a negative sideforce.

At $\phi_s = 90$ deg, however, the strake vortex is considerably larger and well displaced from the forebody; the forced separation does not reattach, but forms a saddle point in the wake. Here, the strake may be considered to function as a spoiler creating an effective circulation in the opposite direction (see Ref. 5). The "strake-vortex" mechanism (A) would be expected to produce significant side force primarily in the intermediate alpha range where stable forebody vortices occur, whereas the "spoiler" mechanism (B) would be dominant at angles of attack approaching 90 deg.

The effect of strake deflection is now considered for the case of $\phi_s = 90$ deg. As shown in Fig. 7, a positive (up) deflection of the strake moves the vortex closer to the leeward meridian, where its suction effect delays flow separation on the opposite (i.e., right-hand side) of the forebody, thus producing a positive side force. Conversely, negative (down) strake deflection causes the right-side separation to occur earlier. These systematic effects of strake deflection provide an indication of the side-force modulation capability using a single strake.

The case of dual strake deployment at $\phi_s = 90/270$ deg is presented in Fig. 8. Here, $\delta_s = 0$ deg on either side generating a symmetrical pair of augmented vortices represents the baseline case. Antisymmetric strake deflection (left strake up, right strake down) causes the left vortex to be lifted up while the right vortex is drawn closer to the forebody. The induced asymmetry of pressure distributions on either half is not as marked, however, as with a single strake at $\phi_s = 90$ deg, leading to the expectation that the side-force potential of dual strakes will be comparatively less.

Pressure distributions for a single strake at $\phi_s = 120$ deg are shown in Fig. 9. The strake at this position apparently continues to function as a spoiler, generating a higher level of suction on the opposite side of the forebody. Positive deflection of the strake (up 60 deg) produces an almost equal but opposite effect on either side of the forebody, suggesting an effective side-force modulating capability.

The dual strake case ($\phi_s = 120/240$ deg) is shown in Fig. 10. An antisymmetric deflection (left strake up, right strake down) progressively increases the left-side suction; again, the degree of asymmetry (and consequently the side-force potential) is not as pronounced as with a single strake.

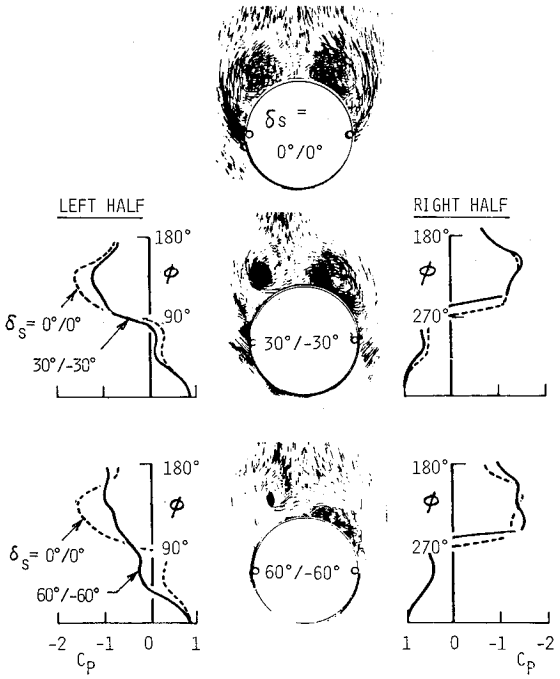

Fig. 8 Flow visualization and pressure distributions with dual strakes at $\phi_s = \pm 90$ deg, showing effect of antisymmetric deflection.

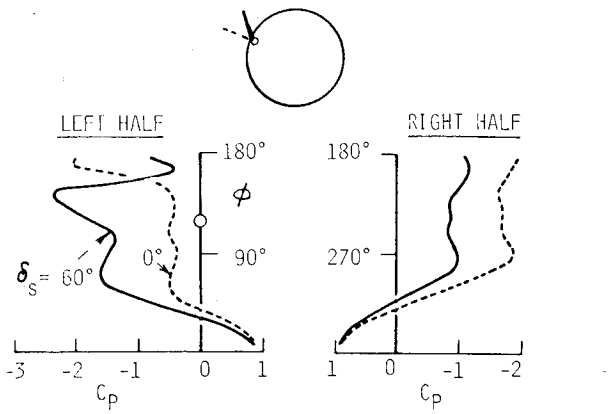

Fig. 9 Pressure distributions with single strake at $\phi_s = 120$ deg, showing effect of deflection.

Flow visualizations in the crossflow plane as well as in side views for the dual strakes ($\phi_s = 120/240$ deg) at $\alpha = 50$ deg are presented in Fig. 11. The vortex from the up-deflected (left) strake is drawn toward the forebody and generates the high suction peaks observed in the left-half pressure distribution. In the side view, this vortex is identified as having a tightly wound core; the relatively diffused vortex from the down-deflected strake is not as readily visualized.

Force and Moment Measurements

Isolated Fuselage

The purpose of these initial tests was to confirm the trends with respect to ϕ_s and δ_s inferred from the pressure surveys and also to assess the yawing moment effectiveness of forebody strakes through an extended angle-of-attack range. The position effect of a single strake with ϕ_s varied at 60–90 deg is shown in Fig. 12. These data (based on the delta wing reference area) confirm the reversal of asymmetry when the strake is moved from $\phi_s = 60$ to 90 deg. Also shown is an intermediate case of $\phi_s = 80$ deg where the yawing moment

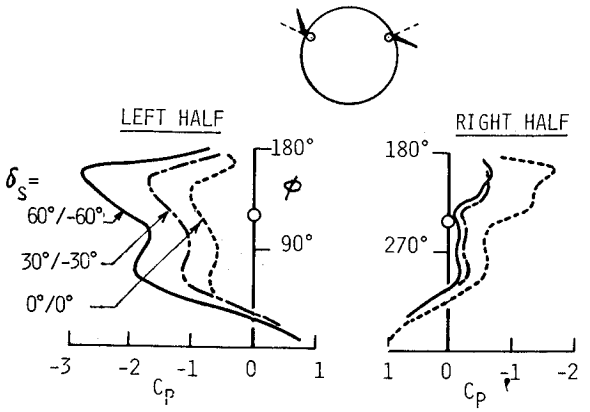

Fig. 10 Pressure distributions with dual strake $\phi_s = \pm 120$ deg, showing effect of antisymmetric deflection.

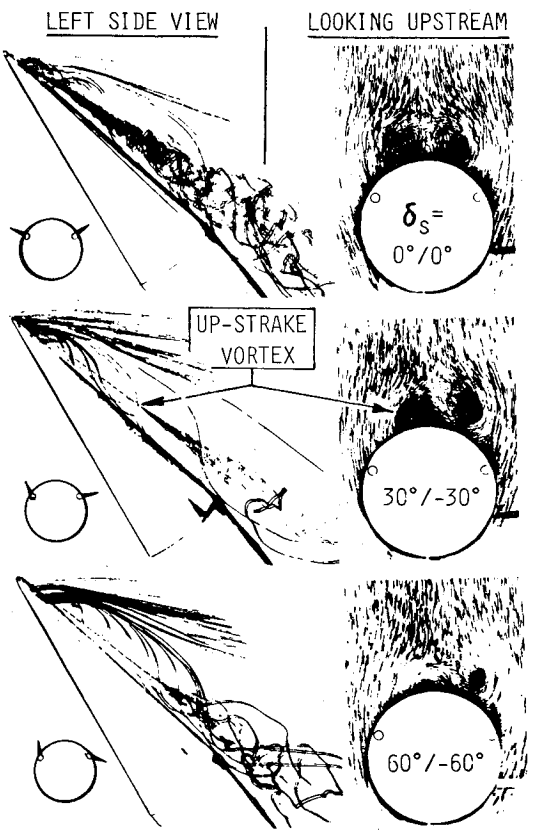

Fig. 11 Side-view and crossflow visualizations with dual strakes at $\phi_s = \pm 120$ deg, showing effect of antisymmetric deflection.

changes direction with increasing angle of attack (presumably as a result of the flow mechanism changing from A to B, making it an undesirable location for single-strake deployment. Although the 60 and 90 deg locations yield comparable yaw power in the intermediate angle-of-attack range, at very high alpha (viz. $\alpha > 60$ deg) the yawing moment capability is better retained with the $\phi_s = 90$ deg strake, lending credence to the hypothesized spoiler flow mechanism B. A weakening of the strake-vortex mechanism A due to the vortex core lifting away from the forebody at higher angles of attack is evident in the case of $\phi_s = 60$ deg.

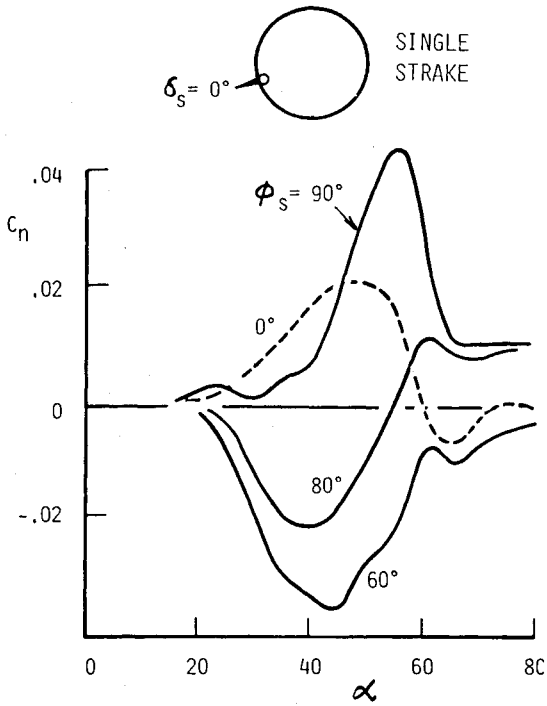

Fig. 12 Yawing moment characteristics of fuselage with single strake at $\phi_s = 60$–90 deg.

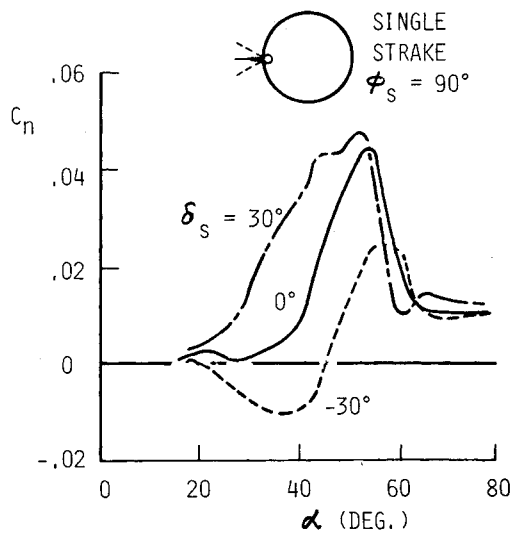

Fig. 13 Yawing moment characteristics of fuselage with single strake at $\phi_s = 90$ deg, showing effect of deflection.

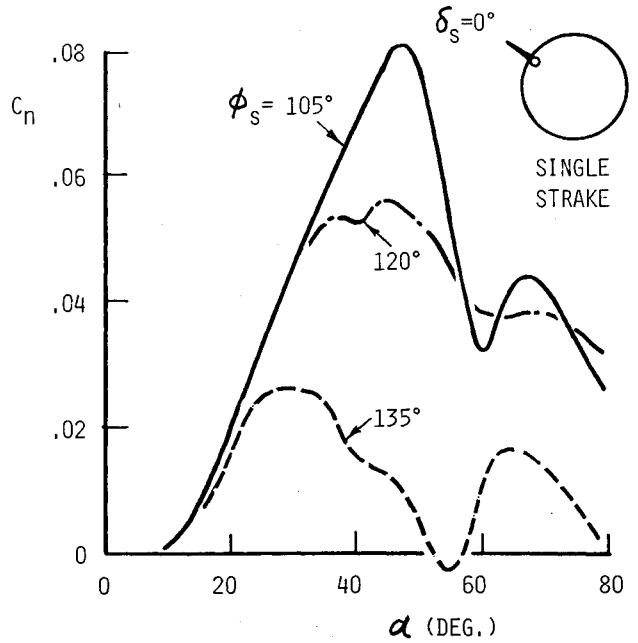

Fig. 14 Yawing moment characteristics of fuselage with single strake at $\phi_s = 120$–135 deg.

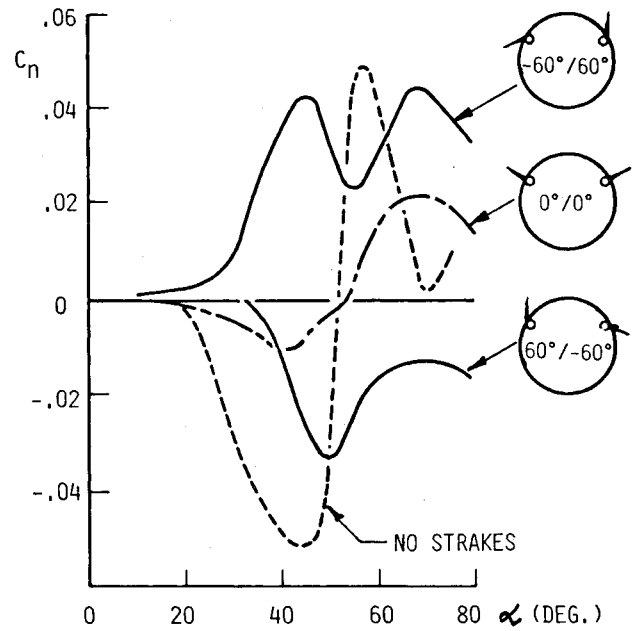

Fig. 15 Yawing moment characteristics of fuselage with dual strakes at $\phi_s = \pm 120$ deg.

The typical effect of strake deflection at $\phi_s = 90$ deg is presented in Fig. 13. Yaw control modulation via strake deflection, which essentially determines the vortex position, might be expected to degrade at the higher angles of attack when the vortex mechanism A is less effective, as confirmed in Fig. 13.

The results with an asymmetric strake at locations $\phi > 90$ deg are presented in Fig. 14. A marked improvement in the high-alpha yawing-moment capability occurs as ϕ_s is increased from 90 to 120 deg, which follows from the greater pressure asymmetry across the forebody observed for this case (see Fig. 9). The case of dual strakes at ϕ_s 120/240 deg is presented in Fig. 15. Included for reference is the basic forebody (i.e., strakes off) yawing moment characteristics, which display asymmetry reversals through the α range. Symmetric dual strakes at zero deflection substantially reduce the asymmetry of the basic forebody, which suggests a significant effect of the strakes on the forebody vortex wake development at high angles of attack. The yaw effectiveness generated in either direction by antisymmetrical strake deflections is sustained to the highest angle of attack (a directional bias probably indicating asymmetrical wake interaction with the aft fuselage). However, the magnitude of yawing moment (as measured from the zero-deflection datum) is only about 50% of that produced by an asymmetrical strake.

Trapezoidal Wing Configuration

The results for a single strake at $\phi_s = 105$ deg have been selected to illustrate the yaw control capabilty on the trapezoidal wing configuration. The yawing moment results

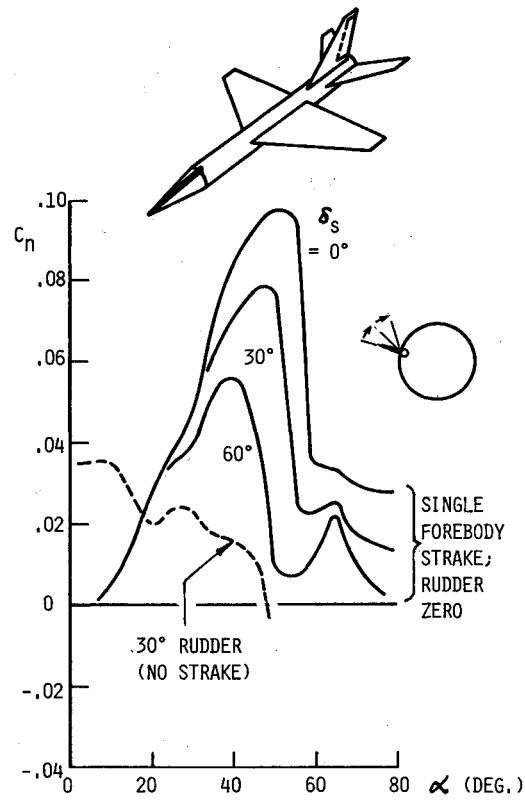

Fig. 16 Yawing moment characteristics of trapezoidal-wing configuration with single strake at $\phi_s = 150$ deg in comparison with rudder.

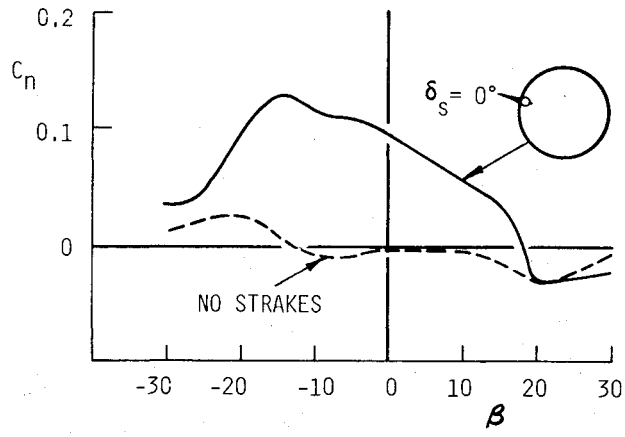

Fig. 17 Yawing moment characteristics in side-slip of trapezoidal-wing configuration with single strake at $\phi_s = 105$ deg.

presented in Fig. 16 compare the forebody strake and rudder characteristics. The onset of forebody-strake yaw power coincides with the decline of rudder effectiveness above $\alpha = 10$ deg, reaching a peak value considerably in excess of the low-α rudder power just as the latter is reduced to zero. At $\alpha > 50$ deg, the strake still continues to generate a yaw power comparable with the rudder at $\alpha = 0$. Also seen is the yaw modulation capability above $\alpha = 30$ and up to 80 deg, the maximum angle of attack of the test.

Since poststall maneuvering usually involves considerable side-slip excursions, yaw control effectiveness at large positive and negative side-slip angles is important. The effect of side slip at a constant 50 deg angle of attack on the yaw control power of the $\phi_s = 105$ deg asymmetric strake is shown in Fig. 17. The yaw control is found to be maintained up to nearly 20 deg of the side-slip angle in either direction.

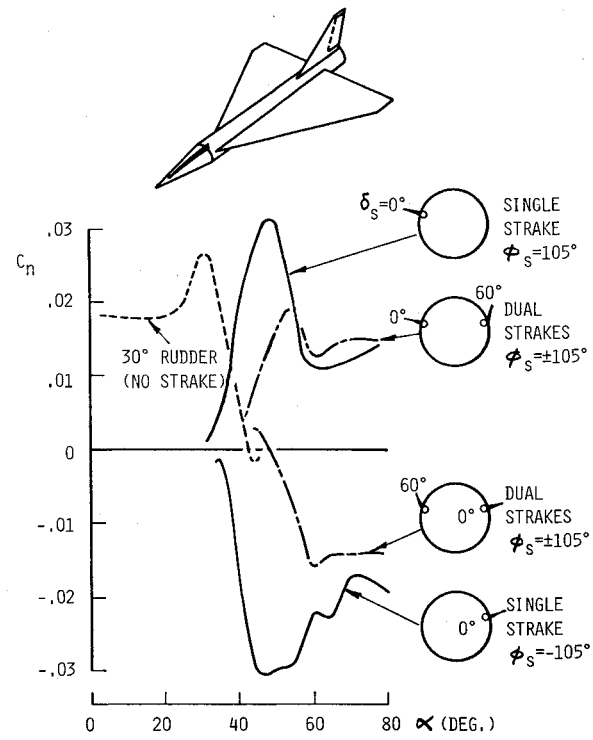

Fig. 18 Yawing moment characteristics of delta-wing configuration with single and dual strakes in comparison with rudder.

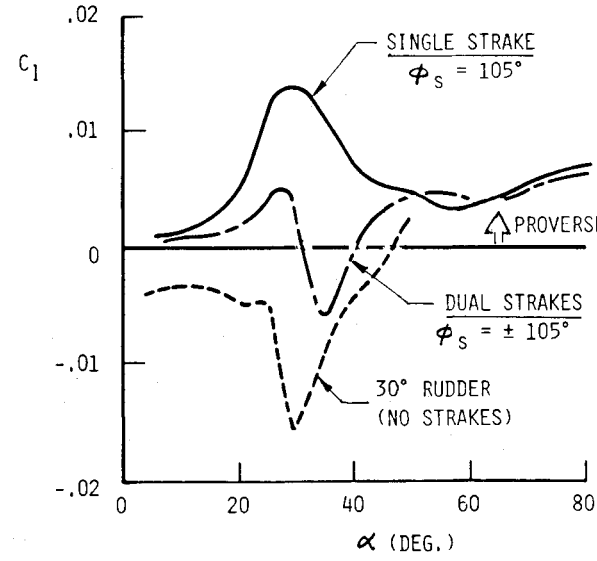

Fig. 19 Induced-roll characteristics of delta-wing configuration with strakes in comparison with rudder.

Delta-Wing Configuration

The change from a trapezoidal to a delta-wing configuration has two geometric effects: the effective forebody length is reduced approximately 50% while the wing reference area is increased by 88%. A forebody length reduction would degrade the aerodynamic effectiveness of yaw strakes; furthermore, the moment coefficient would be reduced due to increased reference area. Still, the strake yaw capability can be assessed in comparison with rudder effectivness on the same configuration. Thus, although the magnitude of the delta-wing yawing moment coefficients shown in Fig. 18 is substantially less than is obtained with the trapezoidal configuration, they remain competetive with the low-α rudder power. A comparison of the single- and dual-strake arrangements again in-

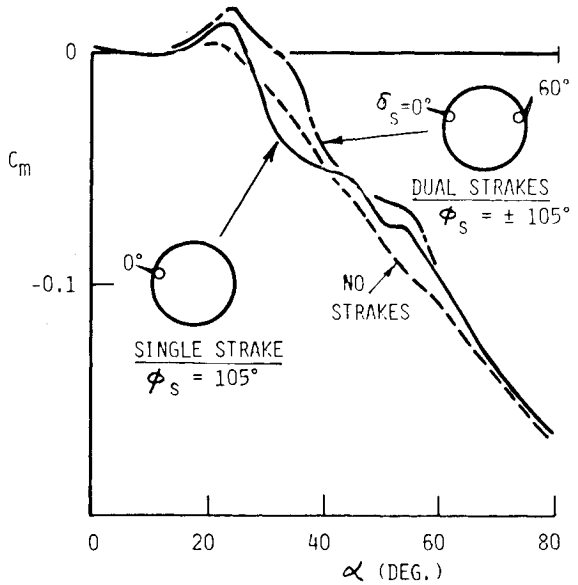

Fig. 20 Pitching moment characteristics of delta-wing configuration with strake deployment.

dicates the former to be more effective for yaw control, certainly in the intermediate (i.e., $\alpha = 40$–60 deg) range.

The induced-roll characteristics are shown in Fig. 19. The rudder produces an adverse rolling moment, whereas the single-strake deployment generates a proverse roll. It is useful to recall that the rudder side force is in opposition to the direction of turn, whereas the forebody side force is proturn. Thus, the indirect effects associated with forebody strake deployment for yaw control should be favorable to high-α handling characteristics. The pitching moment characteristics shown in Fig. 20 indicate a nose-up increment due to strake deployment; however, the induced pitch instability is rather small.

Conclusions

An exploratory low-speed wind-tunnel study was conducted to evaluate a deployable forebody strake concept for yaw control at angles of attack above the effectiveness range of conventional rudder. Flow visualizations and circumferential pressure surveys on an isolated conical forebody were combined with force and moment measurements on generic fighter configurations incorporating the same forebody geometry in order to acquire insights into the forced asymmetric forebody separation and vortex mechanisms and to evaluate the resulting yaw control potential. The variables studied were the circumferential location of the strake on the forebody and strake deflection angle; the data were analyzed for the most advantageous development of side force with angle of attack and for side-force modulation. Furthermore, the relative merits of a single asymmetric strake vs dual strakes were investigated. The flowfield observations suggested plausible flow mechanisms to explain the varying aerodynamic asymmetries produced by different strake arrangements. The force and moment results showed that a single strake, located between 105 and 120 deg from the windward meridian, had considerable yaw control potential in the α range of 20–80 deg; the associated indirect effects in roll and pitch were found to be rather small.

Acknowledgment

This research was jointly supported by the NASA Langley Research Center and the U.S. Air Force Wright Aeronautical Laboratory. The encouragement and support received from Joseph L. Johnson (NASA Langley) and Dieter Multhopp (AFWAL) are greatly appreciated.

References

[1]Hunt, B. L., "Asymmetric Vortex Forces and Wakes on Slender Bodies," AIAA Paper 82-1336, Sept. 1982.

[2]Skow, A. M., Moore, W. A., and Lorincz, D. J., "Forebody Vortex Blowing—A Novel Control Concept to Enhance Departure/Spinning Recovery Characteristics of Fighter and Trainer Aircraft," AGARD CP 262, 1979, Paper 24.

[3]Carr, P. C. and Gilbert, W. P., "Effects of Fuselage Forebody Geometry on Low-Speed Lateral-Directional Characteristics of Twin-Tail Fighter Model at High Angles of Attack," NASA TP 1592, Dec. 1979.

[4]Rao, D. M. and Murri, D. G., "Exploratory Investigation of Deflectable Forebody Strakes for High-Angles-of-Attack Yaw Control," AIAA Paper 86-0333, Jan. 1986.

[5]Lockwood, V. E. and McKinney, L. W., "Effect of Reynolds Number on the Force and Pressure Distribution Characteristics of a Two-Dimensional Lifting Circular Cylinder," NASA TN D-455, Sept. 1960.